

The impact of collective vibrations on quasiparticle states of open-shell odd-mass nuclei and possible interference with tensor force

A. V. Afanasjev¹ and E. Litvinova^{2,3}

¹*Department of Physics and Astronomy, Mississippi State University, MS 39762*

²*Department of Physics, Western Michigan University, Kalamazoo, MI 49008-5252, USA*

³*National Superconducting Cyclotron Laboratory, Michigan State University, East Lansing, MI 48824-1321, USA*

(Dated: October 27, 2015)

The impact of collective vibrations on quasiparticle states of open-shell odd-mass nuclei and their possible interference with tensor force is investigated. The inclusion of collective vibrations and their coupling to single-quasiparticle motion improves the description of experimental spectra in such nuclei. We found that the energy splittings of the single-quasiparticle states, which are sensitive at the mean field level to the tensor part of the effective nucleon-nucleon interaction, are affected by quasiparticle-vibration coupling. Both quasiparticle-vibration coupling and effective tensor interaction act in the same direction. This suggests that effective tensor interaction has to be quenched as compared with previous estimates.

PACS numbers: 21.10.Jx, 21.10.Pc, 21.60.Jz, 27.70.+j, 27.70.+q

I. INTRODUCTION

The tensor force is known to be one of the important components of the bare nucleon-nucleon interaction. However, it is still an open question whether or not the effective tensor force used in the density functional theory (DFT) framework for medium-mass and heavy nuclei keeps a close resemblance with the original bare tensor force [1]. Moreover, the question of unambiguous signatures of the tensor force remains open [1]. For example, the fits of the energy density functionals (EDF's) to bulk nuclear properties (masses, radii) usually disfavor effective tensor interaction [1]; note that such fits are standard in the DFT. On the other hand, some possible indications of the presence of effective tensor interaction come from the analysis of the spectra of predominantly single-particle states in odd-mass nuclei; they are discussed in detail below. Possible manifestations of effective tensor force in the DFT framework have been recently reviewed in Ref. [1]. Although there is a general consensus that the tensor component has to be added to the DFT [1–7], the question about its strength is still not fully resolved.

Following Ref. [3], there were attempts to find a signature of the effective tensor force in the evolution of the single-particle states along the isotopic or isotonic chains. For example, the energy differences between the proton $1g_{7/2}$ and $1h_{11/2}$ quasiparticle states in the Sb ($Z = 51$) isotopes and the neutron $1i_{13/2}$ and $1h_{9/2}$ quasiparticle states in the $N = 83$ isotones were considered in Skyrme DFT calculations with the SLy5 functional in Ref. [5]. It was concluded that these energy splittings can be reproduced only when the tensor component is added to the functional. A similar investigation has been performed with the Gogny functionals but only for $N \geq 64$ isotopes in Ref. [8] and lead to the same conclusion. The studies of the Sb isotopes with $N \geq 66$ in Ref. [9] within the relativistic Hartree-Fock approach showed that the relevant energy splittings are only reproduced when the

pion tensor coupling of half of its standard value is included. However, extensive multiparameter minimizations led to the conclusion that the optimal fit to bulk properties of infinite nuclear matter and spherical finite nuclei is achieved for the vanishing pion field, and, thus, no tensor force.

It is necessary to recognize that these DFT studies miss important physics related to the fragmentation of the single-particle states due to coupling with vibrations which is very strong in many nuclei. They assume that above mentioned states are of single-particle nature despite the fact that their fragmentation is supported by numerous experimental observations [10–15]. Thus, mean field studies ignore the realistic structure of the wavefunction of the states and, as a consequence, the fit of the parameters of effective tensor force to their energies can be misleading.

The proper way to proceed is to take into account particle-vibration coupling (PVC) which affects both the wavefunctions and the energies of the states of odd spherical nuclei [16, 17]. However, this has never been done in the context of the study of the effective tensor force because such investigation involves open-shell nuclei in which the pairing correlations of the superfluid type have to be taken into account.

On the other hand, it has been found that in both non-relativistic and relativistic frameworks the PVC improves the description of the energies and wave functions of the levels with dominant single-particle content in odd mass neighbours of doubly magic nuclei. In the relativistic framework this was verified in the systematic studies of single-particle spectra of nuclei neighbouring to ^{56}Ni , ^{132}Sn and ^{208}Pb in Ref. [17] (see Ref. [18] and references therein for non-relativistic results). In addition, Ref. [17] showed for the first time that PVC has an appreciable impact on the energy splittings of the spin-orbit and pseudospin doublets. For example, PVC decreases the splitting of the $1f_{7/2} - 1f_{5/2}$ spin-orbit doublet of ^{56}Ni by approximately 1.5 MeV. This doublet has been used in

the definition of the strength of the tensor interaction in Refs. [6, 7] where the effects of the PVC on its magnitude were neglected.

The question of whether effective tensor force has to be directly included for a proper description of the single-particle spectra and other physical observables is very important, especially in the framework of the CDFT. The absolute majority of very successful applications of CDFT to different physical phenomena have been performed at the Hartree level [19, 20]. However, the inclusion of effective tensor force requires the transition to the Hartree-Fock (HF) level [9, 21]. Unfortunately, this leads to a drastic increase of required computational power, which basically restricts the application of the CDFT at the HF level to the spherical nuclei. The only existing demonstration of such an application to axially deformed nuclei in Ref. [22] has used small basis and showed a requirement for tremendous computational power. In addition, one has to mention that for the absolute majority of physical observables the global descriptions at the Hartree and Hartree-Fock levels are comparable, which definitely indicates that the effects of the Fock term are taken into account at the Hartree level in an effective way during the fit of functional to experimental data.

The main goal of this paper is to understand to which degree beyond mean-field effects (such as the particle-vibration coupling) can modify the conclusions about the role of tensor interaction obtained in the mean field studies. In order to achieve that we have chosen the observables which are known to be sensitive to effective tensor interaction and used for the tuning of its strength. These observables are the energy splittings between the proton $1g_{7/2}$ and $1h_{11/2}$ states in the Sb ($Z = 51$) isotopes and the neutron $1i_{13/2}$ and $1h_{9/2}$ states in the $N = 83$ isotones. These splittings are studied within the relativistic quasiparticle-vibration (RQVC) model developed in Ref. [23].

The paper is organized as follows. Section II describes the details of the calculations. Collective excitations in even-even nuclei are considered in Sec. III. The spectra of ^{116}Sn and ^{148}Dy nuclei obtained in the mean field and quasiparticle-vibration coupling calculations are compared with experimental data in Sec. IV. Sec. V presents the discussion of the energy splittings of the dominant single-particle states sensitive to tensor interaction. Experimental and calculated spectroscopic factors of the states under consideration are compared in Sec. VI. Finally, Sec. VII summarizes the results of our work.

II. THE DETAILS OF CALCULATIONS

The RQVC model [23] employed in the present paper is an extension of the PVC model of Ref. [16] and takes into account pairing correlations of the superfluid type in the quasiparticle-phonon coupling self-energy. Compared to some perturbative approaches to the PVC [18, 24, 25],

which, in fact, remain on the mean-field level and do not include pairing correlations, our model implies an exact solution of the Dyson equation for the single-quasiparticle propagator with a singular frequency-dependent self-energy [16, 23] and includes quasiparticle-vibration coupling (QVC) and pairing on equal footing. These features of our approach allow a proper description of the nuclei of interest. The RQVC model has been successfully tested on the single-particle spectra in proton and neutron subsystems of $^{116,120}\text{Sn}$, in which it substantially improves the accuracy of the description of the spectra as compared with mean field calculations, and applied to superheavy nuclei [23].

The calculations have been performed with the NL3* covariant energy density functional (CEDF) [26]; it is designed at the Hartree level and does not (and not able to) include tensor interaction. This functional represents one of very few relativistic functionals the performance of which has been tested globally with respect of the ground state observables [27] and systematically in the local regions of nuclear chart with respect of other physical observables such as the energies of one-quasiparticle deformed states in actinides [28] and the moments of inertia of even-even and odd mass nuclei [29]. In the context of this paper, it is important that NL3* has been successfully used in the relativistic PVC studies of the spectra of odd spherical nuclei adjacent to doubly magic nuclei (such as $^{100,132}\text{Sn}$) and the impact of PVC on physical observables [17].

For the superfluid pairing correlations, monopole pairing force is used in our calculations. In order to study the dependence of the results of the calculations on the strength of pairing, two types of the parametrizations for the pairing gaps are employed. First, the calculations are performed with empirical pairing gap $\Delta_{emp} = 12/\sqrt{A}$ MeV [30], where A stands for the mass number. Second, the pairing gaps equal to the five-point indicators $\Delta^{(5)}$ [31]

$$\Delta^{(5)}(X) = \frac{(-1)^X}{8} [E(X+2) - 4E(X+1) + 6E(X) - 4E(X-1) + E(X-2)] \quad (1)$$

defined for each nucleus under study from experimental odd-even mass staggerings are also used. Here X stands either for proton Z or neutron N numbers and $E(X)$ is the (negative) binding energy of a nucleus with X particles. As shown in Ref. [31], this indicator provides the best decoupling from the mean-field effects in model calculations. Below, we will refer the corresponding calculations as the “ Δ_{emp} ” and “ $\Delta^{(5)}$ ” ones. The pairing gaps obtained in these calculations are shown in Fig. 1. In the Sn isotopic and $N = 82$ isotonic chains, the Δ_{emp} pairing gaps are close to 1.1 MeV. The $\Delta^{(5)}$ pairing gaps are larger by roughly 0.2 MeV than the Δ_{emp} ones in the Sn isotopes. In the $N = 82$ isotones, the difference $\Delta^{(5)} - \Delta_{emp}$ increases from ~ 0 MeV at $Z \sim 54$ up to ~ 0.5 MeV at $Z = 70$.

In the RQVC calculations the phonon space includes

normal phonon modes of natural parity and it is truncated by the angular momenta of the phonons at $J^\pi = 6^+$ and by their frequencies at 15 MeV. Further extension of the phonon space does not affect the results. Other limitations of the approach are discussed in Ref. [23].

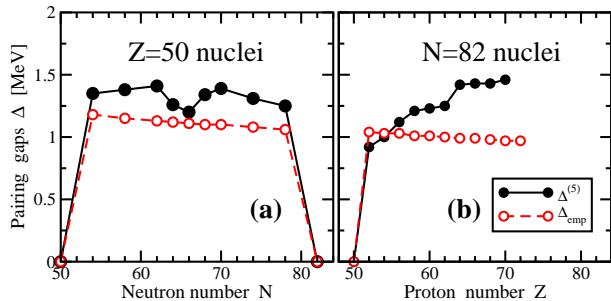


FIG. 1. (Color online) Pairing gaps used in the calculations as a function of particle number. The $\Delta^{(5)}$ pairing gaps are extracted using experimental binding energies from Ref. [32].

III. COLLECTIVE EXCITATIONS IN EVEN-EVEN NUCLEI

Before considering the energy splittings of specific pairs of the states in odd-mass nuclei, it is necessary to understand how well the excitations energies and the electric multipole decay rates of the lowest vibrational states in the Sn and $N = 82$ even-even nuclei are reproduced in the Relativistic Quasiparticle Random Phase Approximation (RQRPA). These characteristics play a decisive role in the RQVC model: the nucleonic self-energy is a function of the phonons' frequencies and quasiparticle-phonon coupling vertices (see, for instance, Eq. (5) of Ref. [23]) while the latter are directly related to the decay rates. Thus, the accuracy of their description defines the quality of the description of the states with significant single-particle content in odd-mass nuclei. The excitation energies of the lowest 2^+ and 3^- states and the corresponding reduced transition probabilities are shown in Figs. 2 and 3, respectively.

The experimental 2^+ energies of the Sn isotopes are better reproduced in the “ Δ_{emp} ” calculations, while the 3^- ones are better described in the “ $\Delta^{(5)}$ ” calculations (see Figs. 2a and c). The experimental reduced $B(E2)$ transition probabilities are slightly better described in the “ $\Delta^{(5)}$ ” calculations (Fig. 3a), while comparable accuracy of the description of experimental reduced $B(E3)$ transition probabilities is achieved in both calculations (Fig. 3c). The level of agreement with experiment obtained in the current calculations is at least comparable with the one obtained in earlier relativistic [33] and non-relativistic [34] QRPA calculations for the Sn isotopes.

Apart of the $Z = 58, 60$ nuclei, the excitations energies of the 2^+ states in the $N = 82$ isotones are reasonably well reproduced in the model calculations (Fig. 2b). The

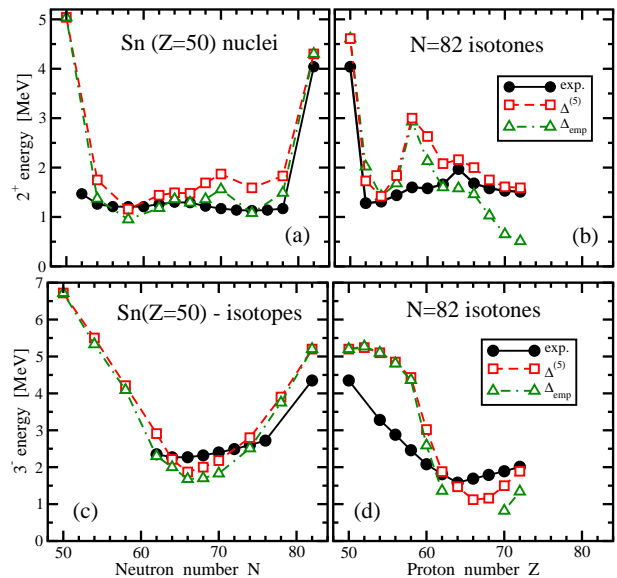


FIG. 2. (Color online) The excitation energies $E(2^+)$ (top row) and $E(3^-)$ (bottom row) of the lowest 2^+ and 3^- states in Sn nuclei (left column) and $N = 82$ isotones (right column). The experimental data are taken from Ref. [35]. Note that for the $N = 82$ isotones two-proton drip line is located at $Z = 74$ in the relativistic Hartree-Bogoliubov calculations with the NL3* CEDF [27].

results for $Z = 58, 60$ are affected by too big shell gap at $Z = 58$, which appear in many CEDF's. It was shown in Ref. [21] that ρ -meson tensor coupling can reduce the size of this gap. The results for the reduced $B(E2)$ transition probabilities are, nevertheless, close to experiment (Fig. 3b). Experimental excitation energies of the 3^- states are overestimated for $Z \leq 58$ (Fig. 2d) because of the same reason as the 2^+ energies, and only above this neutron number the results of the calculations come close to experimental data. It turns out that for the case of “ Δ_{emp} ” pairing the QRPA calculations of the 3^- excitations in the $Z = 64, 66$ and 68 $N = 82$ isotones lead to the appearance of the Goldstone modes (the stability matrix is not positively defined). Only for the pairing strength larger than some critical value the energies and the $B(E3)$ values of the lowest 3^- states have physical magnitudes. The critical value for the pairing gap is larger than the “ Δ_{emp} ” for the nuclei with $Z = 64 - 68$. Therefore, no meaningful calculations can be done for them within the RQVC model.

IV. SPECTRA OF ^{116}Sn AND ^{148}Dy

The examples of the impact of quasiparticle-vibration coupling on the spectra of odd-mass nuclei are shown in Figs. 4 and 5. In these figures, the column “RMF” shows the single-quasiparticle spectra obtained in spherical RMF calculations of even-even nuclei. The dominant levels (i.e. the levels with the largest spectroscopic fac-

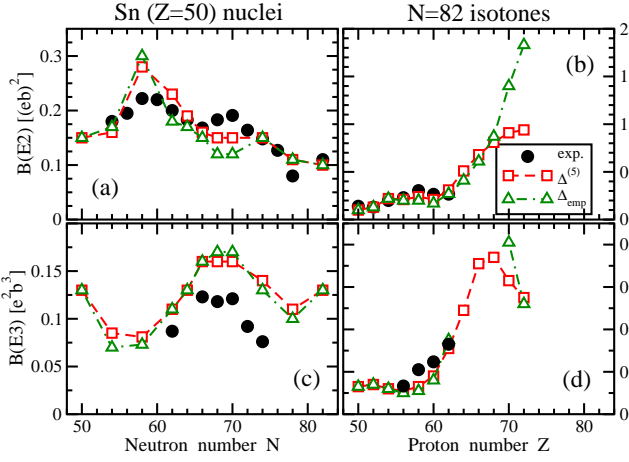


FIG. 3. (Color online) Reduced transition probabilities $B(E2; 0_{gs}^+ \rightarrow 2_1^+)$ (top row) and $B(E3; 0_{gs}^+ \rightarrow 3_1^-)$ (bottom row) for Sn nuclei (left column) and $N = 82$ isotones (right column). The experimental data are taken from Refs. [35, 36].

tors) as obtained in the RQVC calculations are shown in column RQVC. These results are compared with experimental energies of the dominant particle [$\varepsilon(\text{particle})$] and hole [$\varepsilon(\text{hole})$] states closest to the Fermi level determined from the difference of the binding energies of the even-even core [$B(\text{core})$] and the corresponding adjacent odd nuclei [$B(\text{core} + \text{nucleon})$ and $B(\text{core} - \text{nucleon})$] according to Refs. [37, 38] as

$$\varepsilon(\text{particle}) = B(\text{core}) - B(\text{core} + \text{nucleon}) \quad (2)$$

and

$$\varepsilon(\text{hole}) = B(\text{core} - \text{nucleon}) - B(\text{core}). \quad (3)$$

These quantities correspond to one-particle removal energies and they are shown in the column labeled as “exp”.

In Figs. 4 and 5 one can see the two effects of the quasiparticle-vibration coupling: (i) the general compression of the spectra leading to a substantially better agreement with experiment and (ii) in some cases the change of the level sequences. For some of the states, the QVC effect is quite substantial leading to a 2-3 MeV correction in the energy. These are, for example, neutron $1i_{13/2}$, $3p_{1/2}$ and $3p_{3/2}$ states in ^{148}Dy and the proton $2d_{5/2}$, $2d_{3/2}$, $1h_{11/2}$ and $3s_{1/2}$ states in ^{116}Sn . Similar large shifts in energy due to QVC can be found also for the states in proton subsystem of ^{148}Dy and neutron subsystem of ^{116}Sn (see Fig. 4 and 5).

While the mean-field models deal with pure single-particle states, in the RQVC model these states are fragmented due to the coupling to vibrations, in some cases very strongly. However, around the Fermi surface there is often a dominant fragment with a considerable single-particle content. This is in agreement with numerous experimental observations. In this work we discuss only the dominant fragments of the single-quasiparticle states and show that the RQVC model reproduces their fractional occupancies.

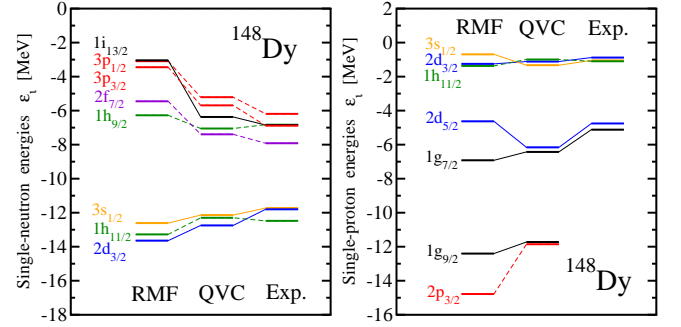


FIG. 4. (Color online) Spectra of ^{148}Dy and its neighboring odd nuclei. Column “RMF” shows the single-quasiparticle spectra obtained in spherical RMF calculations of ^{148}Dy . Column “RQVC” shows the spectra obtained in spherical calculations within the RQVC model and $\Delta^{(5)}$ pairing. Column “exp” shows one-nucleon removal energies defined according to Eqs. (2) and (3); they are based on the data of Refs. [32] (masses of ground states) and Ref. [35] (the energies of excited states). Solid and dashed connecting lines between the states are used to indicate positive and negative parity states.

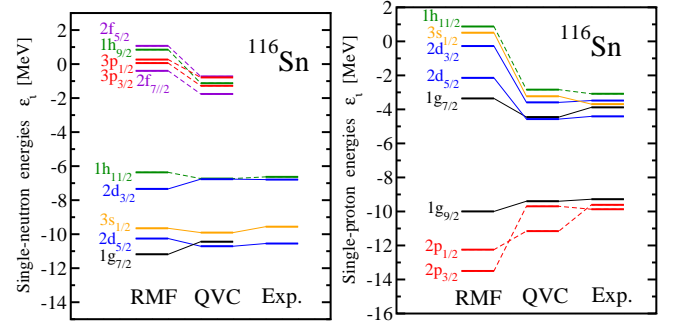


FIG. 5. (Color online) The same as in Fig. 4, but for the spectra of ^{116}Sn .

Figs. 4 and 5 also allow to understand the impact of the QVC on the energy splittings of the pairs of the dominant single-neutron $1i_{13/2}$ and $1h_{9/2}$ states outside the $N = 82$ core and of the dominant single-proton $1h_{11/2}$ and $1g_{7/2}$ states of the Sb isotopes outside $Z = 50$ core. The evolution of these energy splittings along the isotonic/isotopic chains is discussed in details in Sec. V. In each of these pairs of the orbitals, one of the orbitals (neutron $1h_{9/2}$ in ^{148}Dy and proton $1g_{7/2}$ orbital in ^{116}Sn) is only moderately affected by the QVC, while the other orbital (neutron $1h_{13/2}$ in ^{148}Dy and proton $1g_{7/2}$ orbital in ^{116}Sn) is substantially (by about 3 MeV) lowered by the quasiparticle-vibration coupling. As a result, the energy splittings between these pairs of the orbitals are much smaller in the RQVC calculations as compared with mean field values.

V. THE ENERGY SPLITTING OF THE DOMINANT SINGLE-PARTICLE STATES SENSITIVE TO TENSOR INTERACTION

In experiment, the energy splitting $\Delta\epsilon_\pi = \epsilon(\pi h_{11/2}) - \epsilon(\pi g_{7/2})$ between the lowest states of the Sb isotopes corresponding to the two nodeless single-proton $h_{11/2}$ and $g_{7/2}$ orbitals outside the closed $Z = 50$ core gradually decreases in the $N = 54 - 62$ isotopes and then rapidly increases for $N \geq 62$ (Fig. 6a). The change of the energy splitting $\Delta\epsilon_\pi$ on going from $N = 62$ to $N = 82$ is substantial (around 2.5 MeV). The CDFT calculations (performed at the mean field level) give $\Delta\epsilon_\pi \sim 4$ MeV which is smoothly increasing with neutron number.

One can see from Fig. 6 that a large part of the corrections to the energy splittings and, in a half of the cases, the whole effect comes from the QVC. Indeed, the experimental $\Delta\epsilon_\pi$ splitting and its trend with neutron number is reasonably well reproduced in the RQVC calculations for the $N \geq 68$ Sb nuclei. Even in lighter nuclei the QVC improves the agreement between theory and experiment as compared with the CDFT results. Note that dependence on the pairing gaps in the calculations for the $\Delta\epsilon_\pi$ and $\Delta\epsilon_\nu$ splittings is relatively small (Fig. 6). However, on going from $N = 66$ to $N = 50$ this improvement due to QVC is not sufficient to fully reproduce experimental trend. This is consistent with the behaviour of the energies of the first octupole states for small neutron numbers and also points out to the increase of the importance of other mechanisms than those included into the RQVC model. For example, isospin and pairing vibrations are usually not included in the RQVC phonon basis, however, their contribution can be important and should be studied in the future.

Unfortunately, the studies of the pion tensor coupling in CDFT in Ref. [9] and tensor interaction in Gogny DFT in Ref. [3] do not cover the Sb isotopes with $N = 50 - 64$. As a result, it is not clear whether the accounting of these tensor couplings will improve the description of the $\Delta\epsilon_\pi$ splittings for these nuclei. The full $N = 50 - 82$ range is covered only in Skyrme DFT studies of Ref. [5] in which the tensor interaction is added to the Skyrme SLy5 functional. However, similar to our RQVC studies, the experimental $\Delta\epsilon_\pi$ splittings are described rather well only in $N \geq 70$ nuclei, and the discrepancy between theory and experiment is around 1 MeV for lighter nuclei.

A similar situation is seen in the energy splitting $\Delta\epsilon_\nu = \epsilon(\nu i_{13/2}) - \epsilon(\nu h_{9/2})$ of the single-neutron $i_{13/2}$ and $h_{9/2}$ states outside the $N = 82$ core (Fig. 6b). In the Skyrme DFT, this splitting is reasonably well reproduced by the inclusion of the tensor interaction [5] in high- Z nuclei but the discrepancy between theory and experiment increases for $Z \leq 60$. The CDFT mean-field calculations do not reproduce the observed splittings, but the accounting of the QVC improves the description of the experimental $\Delta\epsilon_\nu$ values with the biggest improvement seen in the middle of the shell (Fig. 6b). Similarly to the case of the Sb isotopes, Figs. 2b, d and 6b show

that the best agreement between experiment and theory for the $\Delta\epsilon_\nu$ is achieved for the nuclei in which the calculated excitation energies of the lowest 2^+ and 3^- states are close to experimental ones. Thus, the improvement in the description of these physical observables should improve the description of the splittings.

The comparison of our RQVC results with the DFT ones obtained with non-relativistic Skyrme [5] and Gogny [8] functionals as well as relativistic [9] functionals indicates that both RQVC and tensor interaction act in the same direction and reduce the discrepancies between theory and experiment for the $\Delta\epsilon_\pi$ and $\Delta\epsilon_\nu$ splittings. If to consider both effects combined, the strong impact from RQVC on the discussed splittings suggests that the effective tensor interaction has to be quenched as compared with earlier estimates.

VI. SPECTROSCOPIC FACTORS OF THE STATES UNDER CONSIDERATION

Fig. 7 shows the spectroscopic factors S of the dominant states under investigation calculated within the QVC model and their evolution with the particle number compared to available data. One can see that near magic shell gaps these states are of predominant single-particle nature ($S \sim 0.8$). However, the spectroscopic factors S of these states decrease on going away from the magic gaps indicating the increased coupling of the single-particle motion with vibrations. These trends correlate with the trends of the excitation energies of the lowest 2^+ and 3^- vibrational states. Indeed, the energies of these vibrational states are the highest for the doubly magic nuclei and they are by a factor 2-3 smaller in open shell nuclei (see Fig. 2). As a result, the coupling with vibrations is weaker in doubly magic nuclei and stronger in open shell nuclei, which results in the reduced spectroscopic factors S of the considered dominant states in the nuclei away from the magic ones. The calculated spectroscopic factors and the general trend of their evolution with particle number (Fig. 7) are not very sensitive to the differences of the pairing gaps $\Delta^{(5)}$ and Δ_{emp} .

It was deduced in Ref. [39] that the states of interest are almost single-particle in nature. Based on these results it was concluded in the DFT framework that proper description of the $\Delta\epsilon_\pi$ and $\Delta\epsilon_\nu$ splittings requires tensor interaction [3, 5, 9]. Recently, an alternative analysis of Ref. [10] has shown that the fragmentation of the $\pi g_{7/2}$ and $\pi h_{11/2}$ states is greater than in the study of Ref. [39]. These results support the conclusions of earlier analysis of Refs. [11, 14, 15] which were in contradiction with Ref. [39]. As compared to the experimental data of Ref. [10], our RQVC calculations reproduce well the experimental spectroscopic factors of the $\pi g_{7/2}$ state in all experimentally studied Sb nuclei and the ones of the $\pi h_{11/2}$ state in the $N = 62, 64$ Sb isotopes (Fig. 7a) and somewhat overestimate the fragmentation of the latter state in the $N = 66 - 74$ Sb isotopes. However, the ^{117}Sb data on the

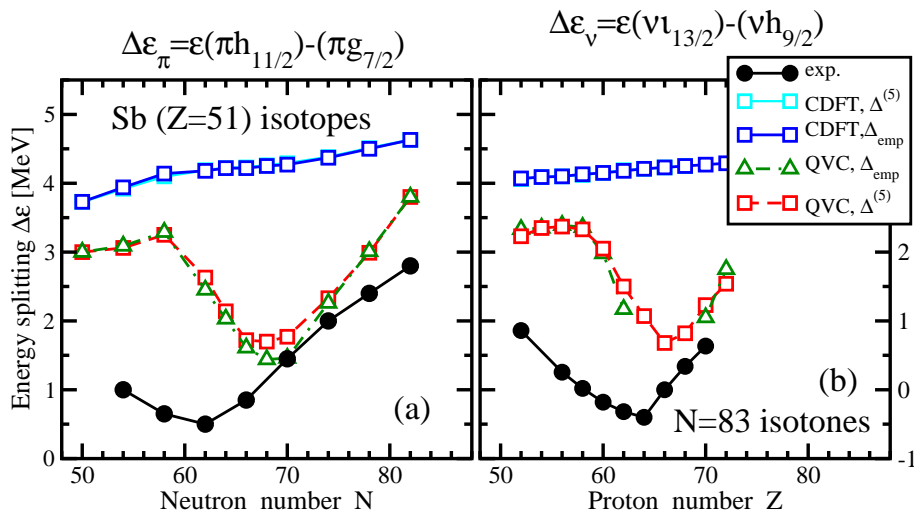


FIG. 6. (Color online) The energy splittings between the indicated states obtained in experiment, covariant density functional theory (CDFT) and RQVC calculations. The results of the calculations with two pairing schemes are shown. Experimental data are taken from Ref. [39].

spectroscopic factors of the $\pi g_{7/2}$ and $\pi h_{11/2}$ states [11] are well reproduced in the RQVC calculations (Fig. 7a). In addition, in agreement with our RQVC calculations the older experimental data of Ref. [14] (see analysis in Ref. [15]) provides low spectroscopic factor $S \sim 0.5$ of the $\pi h_{11/2}$ state in the mid-shell Sb isotopes. Experimental spectroscopic factors depend considerably on the model analysis and on the reaction employed [12, 17]; this fact has also to be taken into account when calculated values are compared with experimental ones. With this in mind one can also conclude that apart of the $h_{9/2}$ state in ^{137}Xe experimental spectroscopic factors of the $\nu i_{13/2}$ and $\nu h_{9/2}$ states in the $N = 83$ isotones are reasonably well reproduced in the RQVC calculations (Fig. 7b). Observed strong fragmentation of the single-particle strength cannot be accounted for at the DFT level. This - again weakens the conclusions of Refs. [3, 5, 9] on the need of strong tensor interaction.

In the context of the current discussion it is interesting to mention that the PVC calculations without pairing based on Skyrme functionals and restricted to odd-mass neighbors of doubly magic even-even nuclei point to either worsening (in ^{40}Ca) or very limited (in ^{208}Pb) improvement of the accuracy of the description of the spectra of such nuclei when tensor interaction is added [18]. Moreover, there are non-relativistic functionals without effective tensor interaction (such as SkM* and SkP) which provide better accuracy of the description of the ^{208}Pb spectra (Ref. [25]) than the functional T44 with tensor interaction used in Ref. [18]. Note also that better accuracy than in T44 functional is achieved in the covariant PVC studies of Ref. [17] with the NL3* CEDF.

VII. CONCLUSIONS

In conclusion, the impact of the quasiparticle-vibration coupling on the energy splitting of specific pairs of the

states in odd-mass nuclei has been investigated in the relativistic framework. We focus on the energy splittings between the proton $1h_{11/2}$ and $1g_{7/2}$ states in the Sb ($Z = 51$) isotopes and the neutron $1i_{13/2}$ and $1h_{9/2}$ states in the $N = 83$ isotones which, according to the earlier studies within the DFT framework, can be described only when effective tensor interaction is introduced. Our analysis unambiguously indicates that both QVC and tensor interaction act in the same direction and reduce the discrepancies between theory and experiment for the $\Delta\epsilon_\pi$ and $\Delta\epsilon_\nu$ splittings. This suggests that the effective tensor force has to be quenched as compared with earlier estimates. These results also show that the definition of the strength of the tensor interaction by means of the fitting to the energies of the dominant single-quasiparticle states in odd-mass nuclei is flawed without accounting for the effects of QVC. For a quantitative analysis of the strength of effective tensor interaction in the density functional theories it is necessary to perform the calculations which incorporate both the quasiparticle-vibration coupling and tensor interaction and, if possible, disentangle explicitly their contributions.

VIII. ACKNOWLEDGEMENTS

This material is based upon work supported by the U.S. Department of Energy, Office of Science, Office of Nuclear Physics under Award Number de-sc0013037, by the U.S. National Science Foundation under the grants PHY-1204486 and PHY-1404343 and by the NSCL.

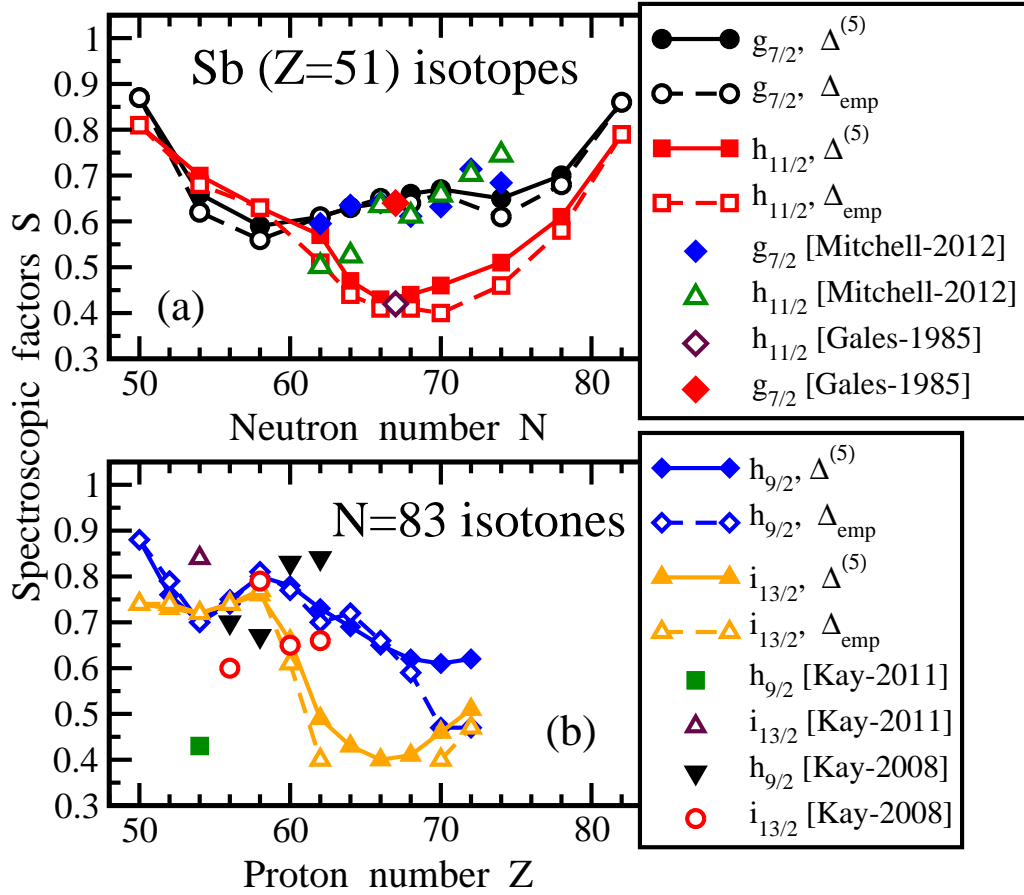


FIG. 7. (Color online) Spectroscopic factors S of the states under study as functions of neutron and proton numbers. Experimental data are taken from Refs. [10] ('Mitchell-2012'), [11] ('Gales-2015'), [12] ('Kay-2011') and [13] ('Kay-2008').

-
- [1] H. Sagawa and G. Coló, *Prog. Part. Nucl. Phys.* **76**, 76 (2014).
- [2] R. J. Furnstahl, J. J. Rusnak, and B. D. Serot, *Nucl. Phys. A* **632**, 607 (1998).
- [3] T. Otsuka, T. Suzuki, R. Fujimoto, H. Grawe, and Y. Akaishi, *Phys. Rev. Lett.* **95**, 232502 (2005).
- [4] T. Lesinski, M. Bender, K. Bennaceur, T. Duguet, and J. Meyer, *Phys. Rev. C* **76**, 014312 (2007).
- [5] G. Coló, H. Sagawa, S. Fracasso, and P. F. Bortignon, *Phys. Lett. B* **646**, 227 (2007).
- [6] M. Zalewski, J. Dobaczewski, W. Satula, and T. R. Werner, *Phys. Rev. C* **77**, 024316 (2008).
- [7] M. Zalewski, W. Satula, J. Dobaczewski, P. Olbratowski, M. Rafalski, T. R. Werner, and R. A. Wyss, *Eur. Phys. J. A* **42**, 577 (2009).
- [8] T. Otsuka, T. Matsuo, and D. Abe, *Phys. Rev. Lett.* **97**, 162501 (2006).
- [9] G. A. Lalazissis, S. Karatzikos, M. Serra, T. Otsuka, and P. Ring, *Phys. Rev. C* **80**, 041301 (2009).
- [10] A. J. Mitchell, PhD thesis "Investigating high- j single-particle energies in $Z = 51$ nuclei", University of Manchester, (available at <https://www.escholar.manchester.ac.uk/item/?pid=uk-ac-man-scw:180683>) (2012).
- [11] S. Gales, C. P. Massolo, S. Fortier, J. P. Schapira, P. Martin, and V. Comparat, *Phys. Rev. C* **31**, 94 (1985).
- [12] B. P. Kay, J. P. Schiffer, S. J. Freeman, C. R. Hoffman, B. B. Back, S. I. Baker, S. Bedoor, T. Bloxham, J. A. Clark, C. M. Deibel, A. M. Howard, J. C. Lighthall, S. T. Marley, K. E. Rehm, D. K. Sharp, D. V. Shetty, J. S. Thomas, and A. H. Wuosmaa, *Phys. Rev. C* **84**, 024325 (2011).
- [13] B. Kay, S. Freeman, J. Schiffer, J. Clark, C. Deibel, A. Heinz, A. Parikh, and C. Wrede, *Phys. Lett. B* **658**, 216 (2008).
- [14] M. Conjeaud, S. Harar, and Y. Cassagnou, *Nucl. Phys. A* **117**, 449 (1968).
- [15] O. Sorlin and M.-G. Porquet, *Prog. Part. Nucl. Phys.* **61**, 602 (2008).
- [16] E. Litvinova and P. Ring, *Phys. Rev. C* **73**, 044328 (2006).
- [17] E. V. Litvinova and A. V. Afanasjev, *Phys. Rev. C* **84**, 014305 (2011).
- [18] L.-G. Cao, G. Coló, H. Sagawa, and P.-F. Bortignon, *Phys. Rev. C* **89**, 044314 (2014).
- [19] D. Vretenar, A. V. Afanasjev, G. A. Lalazissis, and P. Ring, *Phys. Rep.* **409**, 101 (2005).

- [20] T. Nikšić, D. Vretenar, and P. Ring, Prog. Part. Nucl. Phys. **66**, 519 (2011).
- [21] W. Long, H. Sagawa, N. V. Giai, and J. Meng, Phys. Rev. C **76**, 034314 (2007).
- [22] J.-P. Ebran, E. Khan, D. Peña Arteaga, and D. Vretenar, Phys. Rev. C **83**, 064323 (2011).
- [23] E. Litvinova, Phys. Rev. C **85**, 021303(R) (2012).
- [24] G. Coló, H. Sagawa, and P. F. Bortignon, Phys. Rev. C **82**, 064307 (2010).
- [25] D. Tarpanov, J. Dobaczewski, J. Toivanen, and B. Carlsson, Phys. Rev. Lett. **113**, 252501 (2014).
- [26] G. A. Lalazissis, S. Karatzikos, R. Fossion, D. P. Arteaga, A. V. Afanasjev, and P. Ring, Phys. Lett. **B671**, 36 (2009).
- [27] S. E. Agbemava, A. V. Afanasjev, D. Ray, and P. Ring, Phys. Rev. C **89**, 054320 (2014).
- [28] A. V. Afanasjev and S. Shawaqfeh, Phys. Lett. B **706**, 177 (2011).
- [29] A. V. Afanasjev and O. Abdurazakov, Phys. Rev. C **88**, 014320 (2013).
- [30] S. G. Nilsson and I. Ragnarsson, *Shapes and shells in nuclear structure*, (Cambridge University Press, 1995).
- [31] M. Bender, K. Rutz, P.-G. Reinhard, and J. A. Maruhn, Eur. Phys. J. A **8**, 59 (2000).
- [32] M. Wang, G. Audi, A. H. Wapstra, F. G. Kondev, M. MacCormick, X. Xu, and B. Pfeiffer, Chinese Physics **C36** (2012).
- [33] A. Ansari and P. Ring, Phys. Rev. C **74**, 054313 (2006).
- [34] B. G. Carlsson, J. Toivanen, and A. Pastore, Phys. Rev. C **86**, 014307 (2012).
- [35] Evaluated Nuclear Structure Data File (ENSDF) located at the website (<http://www.nndc.bnl.gov/ensdf/>) of Brookhaven National Laboratory. (2014).
- [36] V. M. Bader, A. Gade, D. Weisshaar, B. A. Brown, T. Baugher, D. Bazin, J. S. Berryman, A. Ekström, M. Hjorth-Jensen, S. R. Stroberg, W. B. Walters, K. Wimmer, and R. Winkler, Phys. Rev. C **88**, 051301(R) (2013).
- [37] K. Rutz, M. Bender, P.-G. Reinhard, J. A. Maruhn, and W. Greiner, Nucl. Phys. A **634**, 67 (1998).
- [38] V. I. Isakov, K. I. Erokhina, H. Mach, M. Sanchez-Vega, and B. Fogelberg, Eur. Phys. J. **A14**, 29 (2002).
- [39] J. P. Schiffer, S. J. Freeman, J. A. Caggiano, C. Deibel, A. Heinz, C.-L. Jiang, R. Lewis, A. Parikh, P. D. Parker, K. E. Rehm, S. Sinha, and J. S. Thomas, Phys. Rev. Lett. **92**, 162501 (2004).